Possible shears bands in ^{204}At and ^{206}Fr, and identification of excited states in ^{205,207}Fr

D. J. Hartley and E. P. Seyfried
Department of Physics, U.S. Naval Academy, Annapolis, Maryland 21402, USA

W. Reviol, D. G. Sarantites, C. J. Chiara,* and O. L. Pechenaya†
Department of Chemistry, Washington University, St. Louis, Missouri 63130, USA

K. Hauschild and A. Lopez-Martens
CSNSM, IN2P3-CNRS, F-91405 Orsay Campus, France

M. P. Carpenter, R. V. F. Janssens, D. Seweryniak, and S. Zhu
Physics Division, Argonne National Laboratory, Argonne, Illinois 60439, USA
(Received 22 September 2008; published 25 November 2008; corrected 1 December 2008)

Neutron-deficient astatine and francium nuclei were produced in the reaction $^{30}\mathrm{Si} + {}^{181}\mathrm{Ta} \rightarrow {}^{211}\mathrm{Fr}^*$ at 152 MeV. The evaporation residues from this very fissile system were selected with the HERCULES-II detector system and residue-gated γ rays were measured with Gammasphere. Excited states were observed for the first time in ^{205,207}Fr, as well as sequences of low-energy transitions between high-spin states in ^{204}At and ^{206}Fr. These latter structures have properties similar to those associated with magnetic rotation (shears bands) in lead nuclei. Comparisons with established shears bands are presented and prospects for the magnetic-rotation phenomenon near the predicted $N = 120$ "magic" number are explored.

DOI: 10.1103/PhysRevC.78.054319 PACS number(s): 21.10.Pc, 23.20.Lv, 27.80.+w

I. INTRODUCTION

Relatively little information is known about excited states in the neutron-deficient trans-lead region of nuclei. Indeed, for many isotopes, only the ground state and perhaps an isomeric state have been identified. This is largely due to the low evaporation-residue (ER) cross section in fusion reactions that cannot compete with the fission cross section in this region. The resulting background of γ rays emitted from the fission products makes γ-ray spectroscopy of ER products very difficult, particularly for short-lived high-spin states. It is highly desirable to tag the γ rays associated with the ER channels and improve the peak-to-background ratio for the transitions of interest. A solution to this problem is provided by an ER detector like the 64-element HERCULES device [1]. The combination of HERCULES with Gammasphere [2] has proven to be a powerful means to investigate nuclei where the cross section for fission is about 100 times larger than for the ER channels of interest [3].

In the present experiment, the $^{211}_{87}$Fr compound nucleus was produced leading to ER products of francium, radon, and astatine. The observed nuclei have neutron numbers near $N = 120$, which is relatively close to the $N = 126$ spherical shell gap, and are located midway between the $Z = 82$ shell gap and the $Z = 92$ subshell closure. For the former reason, the nuclei are expected to have rather low deformations and, thus, exhibit vibrational-like energy level sequences as spin increases. However, $N = 120$ has also been postulated to be a "magic" number for so-called magnetic rotation [4,5], which is associated with high-j valence nucleons in a weakly deformed system. The shears bands resulting from magnetic rotation are level structures that exhibit a smooth increase in the γ-ray transition energy with spin, have markedly strong magnetic dipole transitions, and display weak or absent electric quadrupole transitions.

The tilted-axis cranking (TAC) model of Frauendorf [4] provided the first explanation of these bands. In its lowest configuration, the high-j protons and neutrons are coupled with their respective angular momentum vectors perpendicular to each other. The coupling creates a total angular momentum vector that does not lie on any of the principal axes. As excitation energy is increased, the proton and neutron vectors close on the total angular momentum vector (like a pair of shears closing) that increases the spin of the system. The closing mechanism is quantized and, thus, produces spectra similar to collective rotation. A more recent explanation [6] suggests a residual interaction between the high-j protons and neutrons may be the mechanism behind shears bands. This depiction has the advantage of not requiring any deformation in the nuclear system for shears bands to occur.

Shears bands have been well-studied in the lead region as $Z = 82$ was predicted to be a "magic" number for magnetic rotation; see Refs. [5,7] and references therein. Although $Z = 82$ is an established benchmark for shears bands (with 12 lead isotopes exhibiting this phenomenon), the predicted $N = 120$ "magicity" has yet to be fully explored. This is directly attributable to the difficultly of producing high-spin states in the trans-lead region as discussed above. Well above lead, there is only a single sequence in $^{205}_{86}\mathrm{Rn}_{119}$ that has been interpreted as a possible shears band [8]. In the present experiment, the

*Present address: Nuclear Engineering Division, Argonne National Laboratory, Argonne, IL 60439, USA.

†Present address: Department of Radiation Oncology, Washington University School of Medicine, St. Louis, MO 63130, USA.

odd-odd $N = 119$ isotones $^{204}_{85}$At and $^{206}_{87}$Fr have been found to exhibit sequences that appear to be good candidates for the shears mechanism. These structures, along with the first excited states observed in ^{205,207}Fr, are discussed in this article.

II. EXPERIMENT AND ANALYSIS DETAILS

The neutron-deficient nuclei were produced with the ^{30}Si + ^{181}Ta reaction, where the ^{30}Si beam was accelerated to an energy of 152 MeV using the ATLAS accelerator at Argonne National Laboratory and the ^{181}Ta target had a surface density of 0.99 mg/cm^2. The beam intensity was ∼2 pnA. The beam-target combination produces a ^{211}Fr compound nucleus with a high probability for fast fission. However, it is the ER events that were of interest and estimated to account for $\lesssim$2% of the fusion cross section.

In this experiment, an improved version of HERCULES (where the photomultiplier readout is in air) called HERCULES-II [9] was used for the first time. The reaction products were detected at polar angles of $9.7^\circ \leqslant \theta \leqslant 26.8^\circ$ (where $\theta = 0^\circ$ corresponds to the beam axis). Two parameters were measured with HERCULES-II: the time-of-flight (TOF) of reaction products and scattered beam as well as the pulse height (PH) of the signal from each detector element. However, a hardware-veto based on the radio frequency of the accelerator was applied to the events from elastically scattered beam particles, fission products, and certain target recoils to reduce data acquisition deadtime. Figure 1 displays a sample two-dimensional projection of the PH versus TOF from the HERCULES-II array.

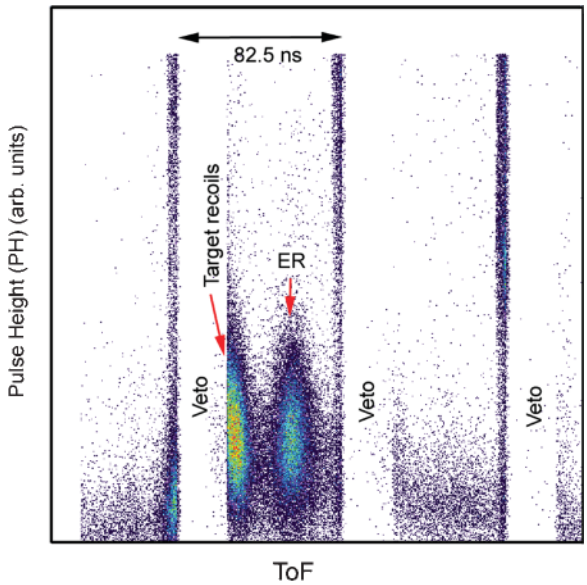

FIG. 1. (Color online) Pulse height versus TOF map for a detector element from ring 3 ($15.5^\circ \leqslant \theta \leqslant 21.2^\circ$) of HERCULES-II. The hardware veto, as described in the text, is clearly displayed in the figure. The scale for the TOF parameter is determined by the ATLAS radiofrequency period of 82.5 ns. The evaporation-residue products and target recoils are also identified in the figure.

The γ radiation from the target was detected with Gammasphere [2], which was composed of 98 HPGe detectors with BGO Compton-suppression shields. Five of the HPGe detectors did not have the hevimet collimators installed because of geometrical constraints. Each HPGe detector had absorbers of 0.05-mm tantalum and 0.25-mm copper at the front face. The Gammasphere timing discriminators were operated in leading-edge mode to enhance detection of low-energy photons. The event trigger was derived from an overlap of logic signals including a HERCULES-II "master" signal, a Gammasphere trigger signal, and a discriminator signal of the accelerator radio frequency. Data were collected for approximately 24 hours.

In the offline analysis, the γ rays from ER nuclei were selected by two-dimensional gating on the TOF and PH parameters. The energies of these γ rays were corrected for the Doppler shifts by using the residue direction observed from the hits of the HERCULES-II elements. The γ-ray energies of coincident transitions were then sorted into an E_γ-E_γ matrix, which contained a total of ∼5 million unfolded γ^2 coincidences. A six-point angular-distribution analysis was performed by gating on all transitions observed in Gammasphere and then measuring the angular dependent intensities, $W(\theta)$, of the strongest transitions. The detectors were grouped into adjacent rings with average angles of 34.6°, 50.1°, 58.3°, 69.8°, 80.0°, and 90.0°. The A_2/A_0 coefficient ratio was determined by a standard Legendre polynomial fit, where the A_4 coefficient was set to zero.

III. LEVEL SCHEMES

Several reaction channels, including $xn, \alpha xn$, and pxn evaporation, were observed; the latter one is of relatively low yield. Element identification for new structures was possible due to the x rays found in coincidence with the γ-ray sequences. In addition, mass assignments were possible in some cases. These assignments are based on the total γ-ray fold (k_γ) distributions[1] for prominent γ-ray transitions and on the results from a cross-bombardment reaction of ^{16}O + ^{197}Au, where the oxygen beam had an energy of 105 MeV [10]. These data were also obtained using HERCULES-II and Gammasphere. As a result, excited states were observed in ^{205}Fr ($6n$ channel) and ^{207}Fr ($4n$ channel) for the first time. The $5n$ and $\alpha 3n$ channels, leading to ^{206}Fr and ^{204}At, respectively, were found to be two of the stronger channels in the data set and their level schemes have been significantly enhanced. The $p4n$ (^{206}Rn [11]) and $\alpha 4n$ (^{203}At [12]) channels were also observed, but no new spectroscopic information was obtained beyond what has been previously reported.

A. ^{205}Fr and ^{207}Fr

Only the ground states of ^{205,207}Fr were previously known from α decay studies as evaluated in Refs. [13,14]. Both ground

[1] Including the hits of both HPGe and BGO elements.

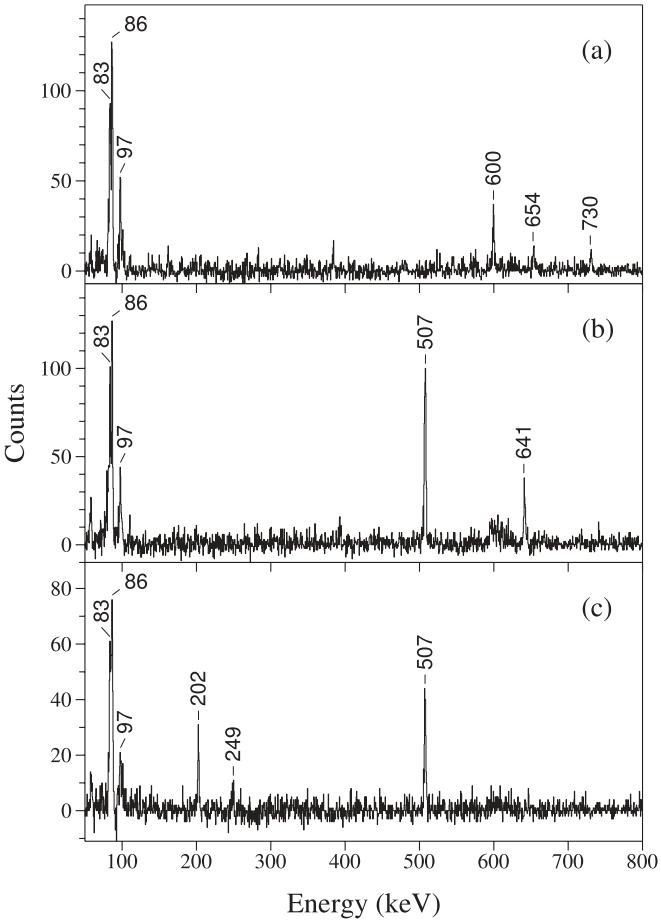

FIG. 2. (a) Transitions in coincidence with the 555-keV γ ray, which have been assigned to ^{207}Fr. (b) Spectrum resulting from a gate on the 503-keV line, which has been placed in ^{205}Fr. (c) Another spectrum displaying transitions in ^{205}Fr where the γ rays are in coincidence with the 778-keV transition.

states were assigned $I^{\pi} = 9/2^{-}$, although this assignment was regarded as tentative for ^{205}Fr. Figure 2 displays sample spectra from structures assigned to ^{205,207}Fr observed in the current data. A coincidence gate placed on the 555-keV transition produced the spectrum in Fig. 2(a). Note the 83-, 86-, and 97-keV x rays, which are the francium $K_{\alpha 2}$, $K_{\alpha 1}$, and $K_{\beta 1}$ lines, respectively. Although the 600-, 654-, and 730-keV transitions were found in coincidence with the 555-keV line, the 654-keV and 730-keV γ rays were not in coincidence with each other. The resulting level scheme is presented in Fig. 3(a), where the ordering of the transitions was based on their intensities, which are given in Table I. This same sequence was found in the $6n$ channel of the $^{16}\mathrm{O} + {}^{197}\mathrm{Au} \rightarrow {}^{213}\mathrm{Fr}^{*}$ experiment, thus, confirming that the structure belongs to ^{207}Fr. The 555-keV transition is clearly quadrupole in nature from its positive A_2/A_0 coefficient, which can be seen in the angular distribution function given in Fig. 4(a), as well as in Table I. However, a slightly negative value was measured for the 600-keV line. This latter transition is a doublet with a γ ray in ^{204}At and, thus, a conclusive assignment cannot be made by the angular distribution. Instead, the spin assignment for the

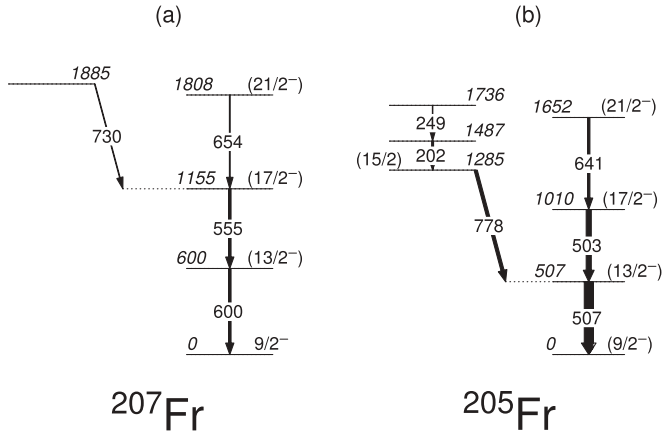

FIG. 3. Proposed level schemes for (a) ^{207}Fr and (b) ^{205}Fr.

first excited state is based on systematics and is addressed in Sec. IV A.

A gate placed on the 503-keV transition is shown in Fig. 2(b), where the francium x rays are observed once again. It is clear that a three-γ-ray sequence was found and is similar to that seen in ^{207}Fr. In addition, a 778-keV line is found in coincidence with the 507-keV γ ray and the spectrum generated by gating on the former is provided in

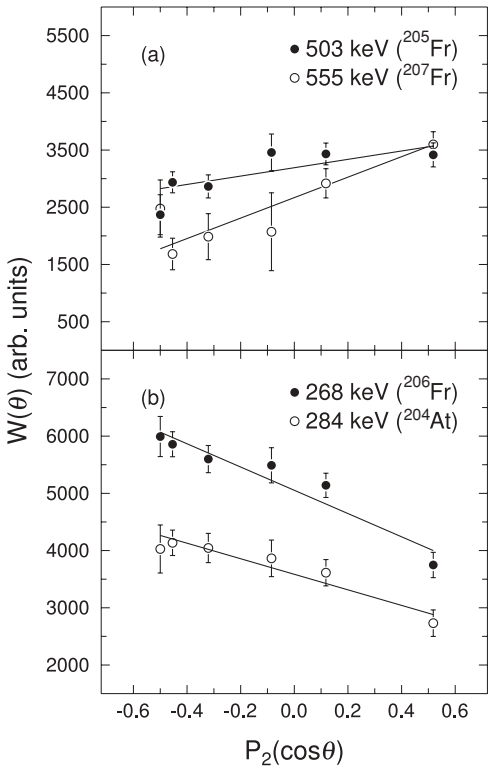

FIG. 4. Sample angular-distribution functions, $W(\theta)$, versus the second-order Legendre polynomial, $P_2(\cos\theta)$, for four strong transitions from the present experiment. In each case, the A_4 parameter was set to zero. Panel (a) displays the 503- and 555-keV γ rays, which are of quadrupole character. Panel (b) displays the dipole transitions of 268 and 284 keV.

TABLE I. Energies, relative intensities, and angular-distribution coefficients for states in ^{205,206,207}Fr and ^{204}At.

^{205}Fr			^{207}Fr		
E_γ (keV)	I_γ[a]	A_2/A_0[b]	E_γ (keV)	I_γ[c]	A_2/A_0[b]
202.2	14(2)		555.2	57(5)	+0.67(12)
249.0	5(1)		599.6	≡100	−0.04(4)[d]
502.9	62(3)	+0.23(8)	653.7	40(8)	
507.4	≡100	+0.28(6)	730.4	20(6)	
641.3	36(2)				
777.6	35(3)	−0.24(9)			
	^{204}At			^{206}Fr	
E_γ (keV)	I_γ[e]	A_2/A_0[b]	E_γ (keV)	I_γ[f]	A_2/A_0[b]
(442.6)[g]			383.5	≡100	−0.04(9)
(496.7)[g]			494.2	40(6)	
490.7	69(4)	+0.20(4)	523.7	68(7)	−0.08(10)
537.4	24(2)		553.1	∼70[h]	−0.71(20)
588.5	11(2)		567.1	∼120[h]	−0.12(8)
600.9	≡100	−0.04(4)[d]	634.4	38(3)	
717.2	31(2)	+0.36(6)	677.7	44(4)	−0.24(14)

[a]Intensities are relative to the 507-keV transition.
[b]The A_4 coefficient was set to zero for each case.
[c]Intensities are relative to the 600-keV transition.
[d]Transition was a part of an inseparable doublet with a group of possibly different multipolarities.
[e]Intensities are relative to the 601-keV transition.
[f]Intensities are relative to the 384-keV transition.
[g]Tentatively assigned to ^{204}At.
[h]Intensity was approximated based on branching ratio and intensity balance considerations.

Fig. 2(c). Two low-energy transitions are found to lie above the 778-keV transition, as seen in Fig. 3(b). The ordering of all the transitions is based on the intensity of the transitions as given in Table I. Positive angular distribution coefficients indicate that the 507- and 503-keV transitions are of quadrupole character [see Fig. 4(a)], whereas the 778-keV line is a dipole transition, which led to the spin assignments given in Fig. 3(b).

This structure was not found in the cross-bombardment reaction; therefore, it must result from a lighter francium isotope than ^{207}Fr. This sequence is not as intense as, nor is it in coincidence with, structures that are assigned to ^{206}Fr (see below). Because the sequence is similar to the levels of ^{207}Fr, we assign these states to ^{205}Fr. In addition, a plot of the aforementioned k_γ distributions for a few of the most intense transitions found in coincidence with francium x rays are presented in Fig. 5. One may deduce from this figure that the 555-keV line (associated with ^{207}Fr) has the highest mean value, and the 507-keV transition (associated with ^{205}Fr) has the lowest one. As more particles are evaporated, the residual nucleus has less excitation energy, which leads (on average) to lower γ-ray multiplicity. Because the 507-keV line has the lowest mean value, it is associated with the channel emitting the most particles. In this case, the 507-keV γ ray is from the $6n$ channel (^{205}Fr) and, thus, the k_γ distributions are consistent with the proposed assignment.

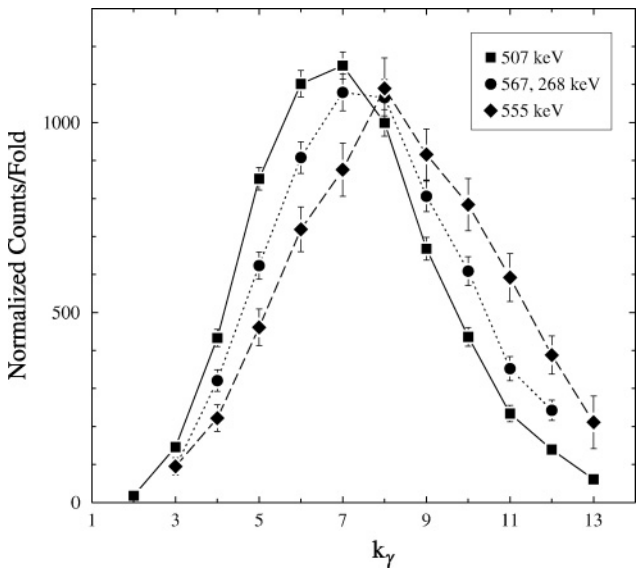

FIG. 5. Total γ-ray fold distributions for prominent transitions identified as francium isotopes. The distribution represented by circles was generated by taking the average of the 567- and 268-keV γ rays. This was necessary as the 567-keV transition was also found as a contaminant line from another nucleus. In addition, the distributions for the 507-keV γ ray were normalized to compare more easily with the other two transitions.

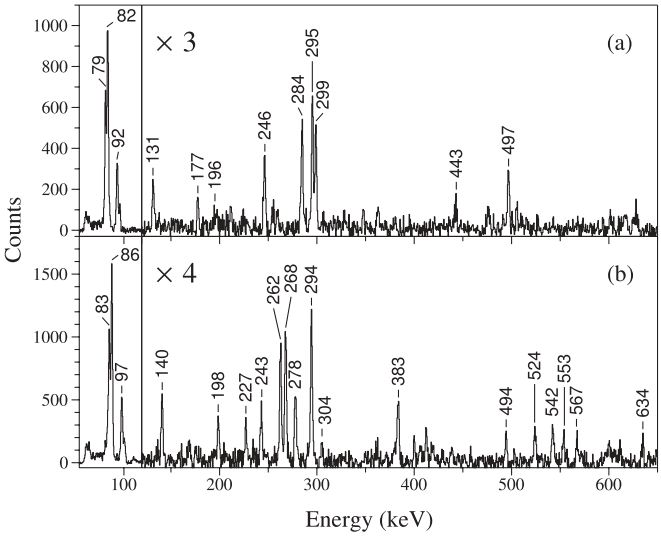

FIG. 6. (a) Summed coincidence spectrum displaying Band 1 in ^{204}At. The spectrum was created by adding the gates from the 131-, 177-, 246-, 284-, and 299-keV transitions. The y scale is reduced by a factor of three above 120 keV. (b) Summed coincidence spectrum displaying Band 1 in ^{206}Fr. The 140-, 198-, 227-, 243-, 262-, 268-, and 278-keV gates were used to produce this spectrum. The y scale is reduced by a factor of four above 120 keV.

B. ^{204}At and ^{206}Fr

The $I^{\pi} = 7^{+}$ ground state and an $I^{\pi} = (10^{-})$ isomeric state ($t_{1/2} = 108$ ms) at 587 keV were previously identified in ^{204}At [15]. In the present experiment, two new structures have been observed which are in coincidence with the astatine x rays. A summed spectrum of one of these bands is found in Fig. 6(a). This spectrum was created by adding the gates on the 131-, 177-, 246-, 284-, and 299-keV transitions. These γ rays (along with the 196- and 295-keV lines) are all mutually coincident and form a sequence of low-energy transitions labeled as Band 1 in the level scheme of Fig. 7(a). The angular-distribution measurements, displayed in Table II with an example given in Fig. 4(b), indicate that these transitions are dipole in character and that they are highly probable to be magnetic dipoles given the large intensity of the x rays observed in coincidence (see Fig. 6). The internal-conversion coefficients for $E1$ transitions are much lower and would produce far fewer x rays than the number observed. The ordering of the transitions in Band 1 could be determined from the total intensity (including the internal-conversion coefficient) of the transitions. The γ-ray energies and intensities for Band 1 are summarized in Table II.

Band 1 is not in coincidence with any of the known transitions in ^{203}At [12] or ^{205}At [16]. However, this structure was weakly seen in the $\alpha 5n$ channel of the cross-bombardment reaction. Therefore, we have assigned this structure to ^{204}At and assume that it is located above the isomeric state, based on the interpretation of the band (see Sec. IV B). This sequence is also in coincidence with the 497- and 443-keV lines [see Fig. 6(a)]. These are likely γ rays from lower-spin states in ^{204}At, perhaps above the 10^{-} isomer; however, there was not sufficient information to create a level structure depicting these transitions.

Another sequence of transitions was found to be in coincidence with astatine x rays, as shown in Fig. 7(a). Once again, none of these transitions were found to have any coincidence relationship with the known γ rays of ^{203}At or ^{205}At. Therefore, we have assigned this sequence to ^{204}At, although Band 1 does not appear to decay into this sequence either. This structure has been placed on top of the $I^{\pi} = 7^{+}$ ground state as a similar sequence is found above the ground

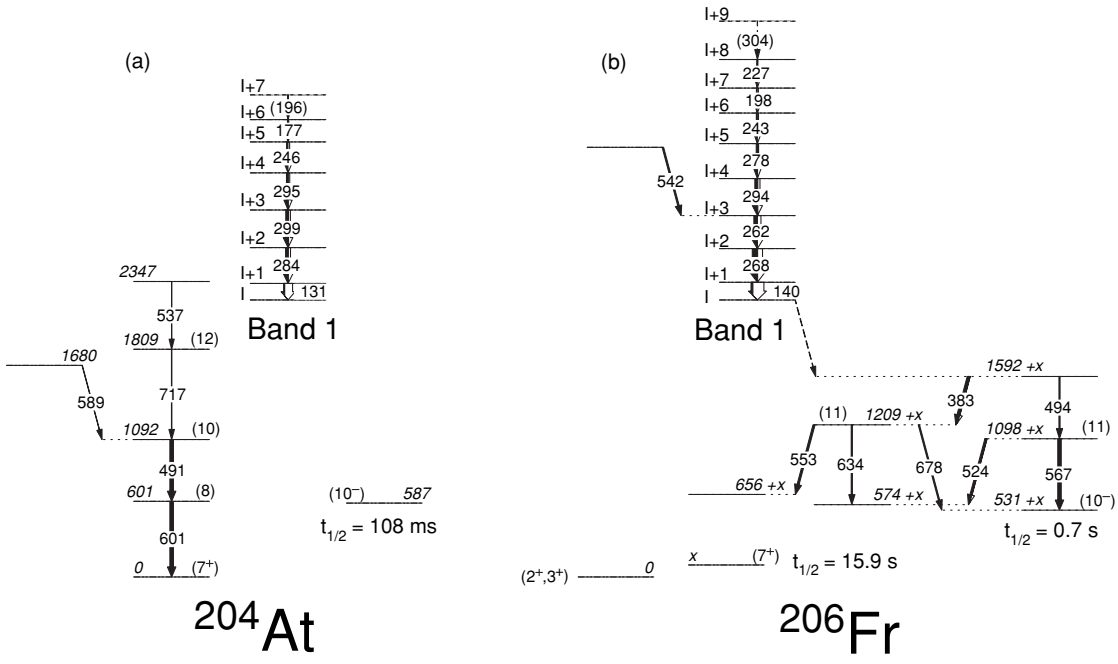

FIG. 7. Proposed level schemes for (a) ^{204}At and (b) ^{206}Fr. The width of the arrows are proportional to the total intensity of the transition.

TABLE II. Energies, relative intensities, angular-distribution coefficients, and $B(M1)/B(E2)$ limits for candidate shears bands in ^{204}At and ^{206}Fr.

E_γ (keV)	I_γ[a]	A_2/A_0[b]	$B(M1)/B(E2)$ $(\mu_N/e\text{b})^2$
		^{204}At	
131.4	34(3)		
177.4	21(2)		>7.7
196.2	<5		
245.9	64(4)	−0.23(8)	>27
284.4	≡100	−0.38(8)	>5.7
295.1	84(5)	−0.44(5)[d]	>34
298.6	87(5)	−0.11(9)	>37
E_γ (keV)	I_γ[c]	A_2/A_0[b]	$B(M1)/B(E2)$ $(\mu_N/e\text{b})^2$
		^{206}Fr	
140.4	36(3)		
198.5	24(2)	−0.76(21)	>10
226.6	22(2)		>8.6
242.6	37(3)	−0.30(12)	>17
262.4	90(4)	−0.41(6)	>17
267.5	≡100	−0.40(5)	>5.9
277.6	56(3)	−0.29(12)	>16
294.1	86(4)	−0.44(5)[d]	>31
304.4	11(1)		>1.5
542.4	35(4)		

[a]Intensities are relative to the 284-keV transition.
[b]The A_4 coefficient was set to zero for each case.
[c]Intensities are relative to the 268-keV transition.
[d]Transition was part of an inseparable doublet.

state in ^{206}At [17]. The nature of the 601-keV line is not clear from the present experiment. However, this line is tentatively assigned to have dipole character, to be consistent with the $E2$ assignment for the 600-keV transition in ^{207}Fr, as discussed above. The 491- and 717-keV γ rays appear to be quadrupoles in nature based on the angular distributions (see Table I).

Only three states were previously assigned to ^{206}Fr [18]. From α-decay studies, a tentative $I^\pi = (2^+, 3^+)$ ground state has been assigned, with a (7^+) isomer located less than 95 keV above the ground state and a (10^-) isomer 531 keV above the (7^+) isomer. The current data produced another sequence of low-energy γ rays; however, this sequence is in coincidence with the francium x rays, as can be seen in Fig. 6(b). This spectrum resulted from a sum of gates on the 140-, 198-, 227-, 243-, 262-, 268-, and 278-keV transitions. These transitions are mutually coincident and form the sequence labeled as Band 1 in Fig. 7(b). Based on arguments similar to those used for Band 1 in ^{204}At, these transitions are also determined to likely have magnetic dipole character. The ordering was once again based on the total intensities. In addition, one may see in Fig. 6(b) that the sequence is in coincidence with several γ rays lying between 350 and 650 keV. Using the coincidence relationships of these transitions, a level scheme could be constructed as displayed in Fig. 7(b). Band 1 feeds into these levels, although no linking transitions were observed. None of these transitions were found in the cross-bombardment reaction, therefore, they result from a francium nucleus lighter than ^{207}Fr. The mean k_γ distribution of the 567- and 268-keV transitions (Fig. 5) lie between the values found for the ^{205}Fr and ^{207}Frγ rays. In addition, the γ rays comprising Band 1 are some of the strongest transitions in the total projection, meaning that it is part of a very strong reaction channel. Because ^{206}Rn$(p4n)$ was the radon isotope most strongly produced and ^{203}At$(\alpha 4n)$ was the most strongly produced astatine, the five-particle channels were clearly favored at the chosen beam energy. With these considerations, it seems highly probable that the structures shown in Fig. 7(b) belong to ^{206}Fr$(5n)$. The vibrational states into which Band 1 feeds have been tentatively placed on top of the 10^- isomer based on arguments to follow (see below).

IV. DISCUSSION

A. ^{205}Fr and ^{207}Fr

Systematics from heavier, odd-A francium nuclei and the neighboring even-even radon and radium nuclei have been used to interpret the observed states. In addition, the systematics of the odd-A astatine states shown in Fig. 8 of Ref. [12] proved useful as well for assigning configurations to the levels.

The $9/2^-$ ground states have been previously interpreted as being based on an unpaired proton in the $h_{9/2}$ state [13]. The first excited state in astatine and francium nuclei near $N = 126$ is typically an $11/2^-$ level with a $13/2^-$ state in close proximity [12,19]. However, the $13/2^-$ state becomes lower in energy with respect to the $11/2^-$ level as the neutron number decreases (see Fig. 8 of Ref. [12]). Both of these states have been interpreted as the $9/2^-$ ground state coupled to the 2^+ excitation of the even-even core [12,19]. Figure 8 plots the 2^+ levels of the radon and radium even-even nuclei, along with the $13/2^-$ states known in ^{209,211,213}Fr [19,20] and the first excited states observed in ^{205,207}Fr. One may conclude that the newly observed states fit in well with the interpretation of these levels being based on the $h_{9/2}$ proton coupled to the 2^+ core excitation.

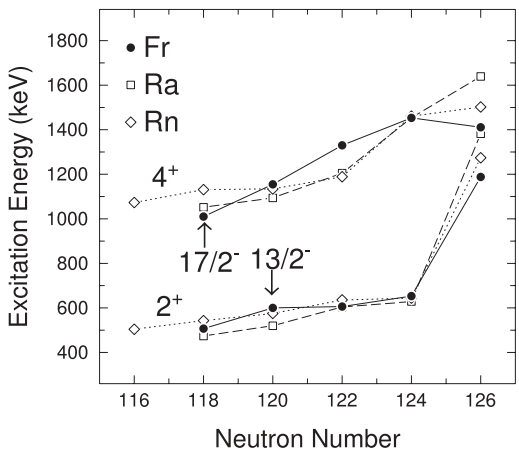

FIG. 8. Energy systematics for the 2^+ and 4^+ states in even-even radon and radium nuclei. In addition, the $13/2^-$ and $17/2^-$ states from neighboring odd-A Fr nuclei are presented.

A similar systematic argument can be applied to the 1010- and 1155-keV states in ^{205}Fr and ^{207}Fr, respectively. By plotting these levels with the known $17/2^-$ states in the heavier francium nuclei and the 4^+ states in the even-even neighbors, as seen in Fig. 8, one may observe the systematic behavior as a function of neutron number. The $17/2^-$ level has been assigned as the $h_{9/2}$ proton coupled to the 4^+ excitation from the even-even core [12,19]. Therefore, this interpretation is given to these states in ^{205}Fr and ^{207}Fr as well.

The next state above the $17/2^-$ levels in the heavier francium nuclei and the astatine isotopes has $21/2^-$ quantum numbers and is associated with the unpaired $h_{9/2}$ proton coupled to the 6^+ excitation [19]. Based on this premise, we have tentatively labeled the 1652-keV and 1808-keV states as $21/2^-$ in ^{205}Fr and ^{207}Fr, respectively. There are no systematic arguments to help interpret the 1885-keV level in ^{207}Fr or the 1285-, 1487-, and 1736-keV states in ^{205}Fr.

B. ^{204}At and ^{206}Fr

With the lack of firm spin/parity assignments and systematic observations from nearby nuclei, it is difficult to provide an interpretation for the collection of levels based on the 7^+ state in ^{204}At or those associated with the 10^- isomer in ^{206}Fr. However, the states labeled as Band 1 for both nuclei in Fig. 7 are of significant interest due to the observation of shears bands in nuclei near $Z \approx 82$ and $N \approx 116$ [5]. As mentioned above, these structures form a rotation-like sequence of magnetic dipole transitions in nuclei with very little deformation. The sequences labeled as Band 1 are reminiscent of the known shears bands in lead and bismuth nuclei [7]. Limits for the corresponding $B(M1)/B(E2)$ ratios can be deduced where the intensity of the $E2$ transition was estimated by fitting the smallest observable peak in the spectrum that was near the energy of the unidentified $E2$ transition. These limits are summarized in Table II where one may see that the ratios are extremely high, some above 30 $(\mu_N/e\text{b})^2$. Such large $B(M1)/B(E2)$ ratios are characteristic of shears bands and these values are comparable to those found in the corresponding ^{198}Pb [21] and ^{199}Pb [22] bands.

Although these structures are similar to known shears bands in terms of strength, they are somewhat different because the spacings of the levels are much less regular than those seen in the lead nuclei. It is interesting to recall that an irregular sequence of low-energy transitions was also reported in ^{205}Rn, an isotone of ^{204}At and ^{206}Fr, and was also suggested to be a shears band [8]. To understand the irregularity, the spins of the states were plotted versus rotational energy[2] in Fig. 9 for these bands in ^{206}Fr and ^{204}At, as well as known shears bands in ^{199,200,202}Bi and $^{197-201}$Pb. Only the spins in the lead nuclei and ^{205}Rn have been determined, whereas assumed spins have been used for the bismuth, astatine, and francium nuclei. In ^{202}Bi, the strongest shears band is found to decay into the shell-model states near spin 12–13$\hbar$ [23]. This, along with the proposed configurations, led Clark *et al.* [23] to suggest a band-head spin of 10–16$\hbar$. We have chosen to display the $N = 119$ bismuth, astatine, and francium sequences with a band-head spin of 15$\hbar$. Any differences from the correct spin will simply shift the data along the ordinate axis.

One may observe in Fig. 9 that for ^{197}Pb and ^{199}Pb (and for lighter lead nuclei that are not shown), a backbend is found in the shears bands near 0.3 MeV. These backbends are the result of an alignment of $i_{13/2}$ neutrons [21,22]. Therefore, the

[2]For $\Delta I = 1$ bands, the rotational energy is simply the energy of the transition depopulating the state.

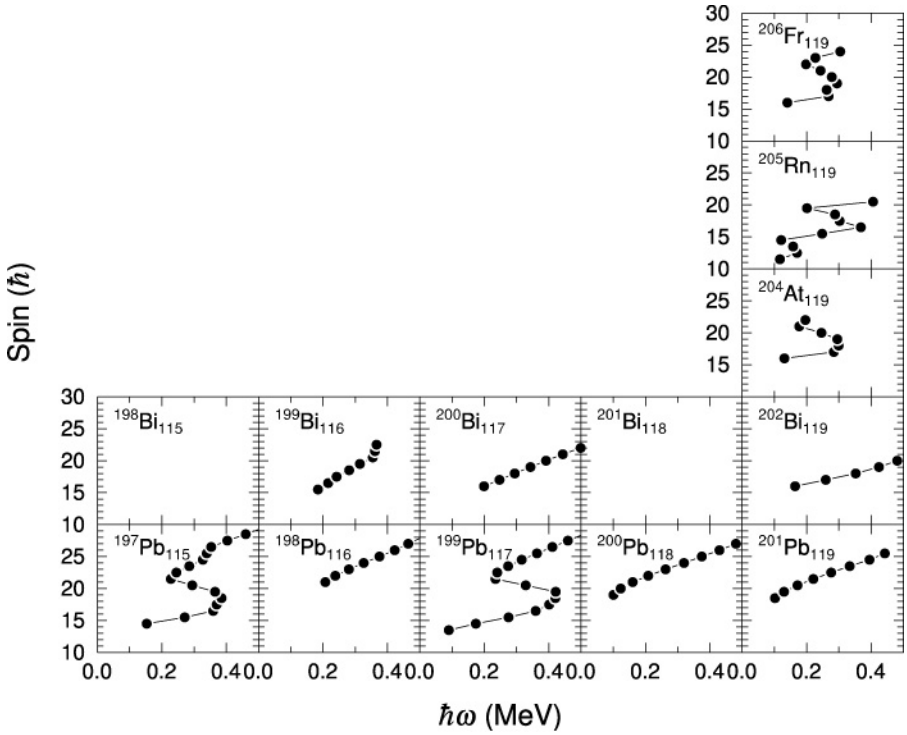

FIG. 9. Plot of spin versus rotational energy for the strongest shears bands in $Z = 82$–87, $N \leqslant 119$ nuclei. The spin of the lowest state for the proposed shears bands in ^{204}At, ^{206}Fr, and ^{200,202}Bi were estimated to be 15$\hbar$.

irregularity seen in the ^{204}At and ^{206}Fr bands is likely caused by a rather low-frequency alignment just above 0.2 MeV. Indeed, if the sequences could be extended to higher spin, the classic rotational spacing of the levels in Band 1 of both nuclei may be observed.

It is interesting to note the difference of the crossing frequencies between the ^{204}At and ^{206}Fr bands and those of the lighter lead nuclei. As mentioned above, the former bands have crossings at a much lower frequency than those seen in the shears bands of the light lead nuclei. This is especially surprising as crossings are not even observed in the heavier ($N \geqslant 118$) lead and bismuth nuclei. The absence of the $i_{13/2}$ neutron alignment in the heavier nuclei is due to the location of the neutron Fermi surface lying high in the $i_{13/2}$ shell near $N = 120$ [24]. Therefore, it takes more energy to break a pair than in the lighter isotopes. For this reason, one might expect that shears bands in the $N = 119$ ^{204}At and ^{206}Fr nuclei would also lack any crossing at low frequencies. Indeed, it is likely that the observed crossing in these isotopes is not from the $i_{13/2}$ neutrons, but instead aligning protons may be responsible for the low-frequency crossing. Such a proton alignment would not be possible at low frequency for nuclei near the $Z = 82$ shell gap, because a large amount of energy would be required to break a pair of protons across the gap. However, at $Z = 85$ and 87, it is possible that a pair of $h_{9/2}$ or $i_{13/2}$ protons could align and cause the observed crossing seen in Fig. 9.

To fully interpret the crossing, the configuration of the bands must be identified. Because neither the spin nor parity of the candidate shears bands in ^{204}At and ^{206}Fr are known, it is not possible to assign a configuration at this time. However, the possible high-j orbitals responsible for these bands may be identified by considering the shears bands closest to ^{204}At and ^{206}Fr. Novak *et al.* [8] suggested that dipole bands based on the $\pi(h_{9/2}, i_{13/2}) \otimes \nu i_{13/2}$ and $\pi i_{13/2}^2 \otimes \nu i_{13/2}$ configurations were predicted to be low in energy for ^{205}Rn according to TRS calculations. In addition, Clark *et al.* [23] proposed that the shears bands in ^{202}Bi$_{119}$ may be based on the 2p-1h proton $(h_{9/2}, i_{13/2}, s_{1/2}^{-1})$ or $(h_{9/2}^2, s_{1/2}^{-1})$ configurations coupled with one or more $i_{13/2}$ neutrons. Therefore, the $h_{9/2}$ and/or $i_{13/2}$ protons along with $i_{13/2}$ neutrons are probably involved in the configuration of the ^{204}At and ^{206}Fr bands. If the low-frequency crossing is indeed associated with an alignment of $h_{9/2}$ or $i_{13/2}$ protons, then the ^{204}At and ^{206} Fr bands involve only a single proton from one of these two high-j orbitals. This single proton may be coupled to three neutrons, where at least one (if not two) come from the $i_{13/2}$ shell. Based on these arguments, it is likely that the shears bands would prefer to decay into levels built above the 10^- isomers in ^{204}At and ^{206}Fr as these long-lived states are associated with the $\pi h_{9/2} \nu i_{13/2}$ configuration.

V. SUMMARY

Excited states were observed in ^{205,207}Fr for the first time and these levels follow the systematics of the heavier francium nuclei. Sequences of low-energy transitions were also found in ^{204}At and ^{206}Fr whose large $B(M1)/B(E2)$ ratios (extracted under reasonable assumptions) make them good candidates for being shears bands. The observation of these bands just one mass unit away from the predicted $N = 120$ "magic" number for magnetic rotation seems to support this prediction. However, because the spins and parities of the band heads could not be assigned, further experimental work is needed to verify the nature of the structures.

ACKNOWLEDGMENTS

Special thanks to D. C. Radford and H. Q. Jin for their software support. The authors thank J. Elson (WU) and J. Rohrer (ANL) for technical support, J. P. Greene (ANL) for the preparation of the target, and F. G. Kondev for useful discussions. This work is funded by the National Science Foundation under grant no. PHY-0554762 (USNA), as well as by the US Department of Energy, Office of Nuclear Physics under contract nos. DE-FG02-88ER-40406 (WU) and DE-AC02-06CH11357 (ANL).

[1] W. Reviol, D. G. Sarantites, R. J. Charity, C. J. Chiara, J. Elson, M. Montero, O. L. Pechenaya, S. K. Ryu, and L. G. Sobotka, Nucl. Instrum. Methods Phys. Res., Sect. A **541**, 478 (2005).
[2] R. V. F. Janssens and F. S. Stephens, Nucl. Phys. News **6**, 9 (1996).
[3] W. Reviol *et al.*, Phys. Rev. C **74**, 044305 (2006).
[4] S. Frauendorf, Nucl. Phys. **A557**, 259c (1993).
[5] R. M. Clark and A. O. Macchiavelli, Annu. Rev. Nucl. Part. Sci. **50**, 1 (2000).
[6] A. O. Macchiavelli *et al.*, Phys. Rev. C **58**, R621 (1998).
[7] Amita Jain, A. K. Jain, and B. Singh, At. Data Nucl. Data Tables **74**, 283 (2000).
[8] J. R. Novak *et al.*, Phys. Rev. C **59**, R2989 (1999).
[9] D. G. Sarantites *et al.* (unpublished).
[10] D. G. Sarantites *et al.* (unpublished).
[11] D. Horn, C. Baktash, and C. J. Lister, Phys. Rev. C **24**, 2136 (1981).
[12] K. Dybdal, T. Chapuran, D. B. Fossan, W. F. Piel, Jr., D. Horn, and E. K. Warburton, Phys. Rev. C **28**, 1171 (1983).
[13] F. G. Kondev, Nucl. Data Sheets **101**, 521 (2004).
[14] M. J. Martin, Nucl. Data Sheets **70**, 315 (1993).
[15] M. R. Schmorak, Nucl. Data Sheets **72**, 409 (1994).
[16] T. P. Sjoreen, D. B. Fossan, U. Garg, A. Neskakis, A. R. Poletti, and E. K. Warburton, Phys. Rev. C **25**, 889 (1982).
[17] X. C. Feng *et al.*, Eur. Phys. J. A **6**, 235 (1999).
[18] F. G. Kondev, Nucl. Data Sheets **109**, 1527 (2008).
[19] A. P. Byrne, G. D. Dracoulis, C. Fahlander, H. Hübel, A. R. Poletti, A. E. Stuchbery, J. Gerl, R. F. Davie, and S. J. Poletti, Nucl. Phys. **A448**, 137 (1986).
[20] G. D. Dracoulis *et al.* (private communication).
[21] A. Görgen *et al.*, Nucl. Phys. **A683**, 108 (2001).
[22] G. Baldsiefen *et al.*, Nucl. Phys. **A574**, 521 (1994).
[23] R. M. Clark *et al.*, J. Phys. G **19**, L57 (1993).
[24] G. Baldsiefen *et al.*, Nucl. Phys. **A592**, 365 (1995).